REPORT DOCUMENTATION PAGE

Form Approved
OMB No. 0704-0188

1. REPORT DATE *(DD-MM-YYYY)*	**2. REPORT TYPE**	**3. DATES COVERED** *(From - To)*
07-21-2011	Final Technical	01/01/2008 - 04/30/2011

4. TITLE AND SUBTITLE

MOLECULAR MACHINE-BASED ACTIVE PLASMONICS

5a. CONTRACT NUMBER

5b. GRANT NUMBER
FA9550-08-1-0349

5c. PROGRAM ELEMENT NUMBER

6. AUTHOR(S)

Tony Jun Huang, J Fraser Stoddart

5d. PROJECT NUMBER

5e. TASK NUMBER

5f. WORK UNIT NUMBER

7. PERFORMING ORGANIZATION NAME(S) AND ADDRESS(ES)

Pennsylvania State University
408 Old Main
University Park, PA 16802

8. PERFORMING ORGANIZATION REPORT NUMBER

9. SPONSORING / MONITORING AGENCY NAME(S) AND ADDRESS(ES)

Air Force Office of Scientific Research
Suite 325, Room 3112
875 Randolph Street
Arlington, VA 22203-1768

10. SPONSOR/MONITOR'S ACRONYM(S)

AFOSR

11. SPONSOR/MONITOR'S REPORT NUMBER(S)

AFRL-OSR-VA-TR-2012-0894

12. DISTRIBUTION / AVAILABILITY STATEMENT

Distribution A - Approved for Public Release

13. SUPPLEMENTARY NOTES

14. ABSTRACT

In the past year, we have made the following significant progress: 1) We demonstrated dual-stimulus switching of a [2]catenane in water. 2) We synthesized mechanically stabilized tetrathiafulvalene radical dimmers. 3) We have developed an efficient technique to fabricate optically thin metallic films with subwavelength patterns and their complements simultaneously. (please refer to Section 2.2. of the final report for more details) 4) We demonstrate a scalable, rapid, and inexpensive fabrication method based on the salting-out quenching technique and colloidal lithography for the fabrication of two types of nanostructures with large electric field: nanodisk dimers and cusp nanostructures. (please refer to Section 2.3. of the final report for more details) 5) We performed Surface Enhanced Raman Spectroscopy (SERS) studies on platinum and gold nanodisk arrays at both plasmon resonant and off-plasmon resonant excitation wavelengths. In addition, we have demonstrated that both surface and resonance Raman enhancement can be exploited to elucidate chemical information in real time about the oxidation state of molecules at an electrode interface. (please refer to Section 3 of the final report for more details) 6) We demonstrated a frequency-addressed plasmonic switch by embedding a uniform gold nanodisk array into dual-frequency liquid crystals (DFLC). (please refer to Section 6.2. of the final report for more details) 7) We carry out a real-time study of all-optical modulation of localized surface plasmon resonance (LSPR) coupling in a hybrid system that integrates a photo-switchable optical grating with a Au nanodisk array. (please refer to Section 6.3. of the final report for more details) 8) We demonstrate dynamic tuning of plasmon-exciton resonant coupling in arrays of nanodisk–J-aggregate complexes. (please refer to Section 6.4. of the final report for more details) 9) We have demonstrated a surface acoustic wave (SAW)-driven light shutter using polymer-dispersed liquid crystals (PDLCs). (please refer to Section 6.5. of the final report for more details)

15. SUBJECT TERMS

16. SECURITY CLASSIFICATION OF:			**17. LIMITATION OF ABSTRACT**	**18. NUMBER OF PAGES**	**19a. NAME OF RESPONSIBLE PERSON**
a. REPORT	**b. ABSTRACT**	**c. THIS PAGE**			Dr. Charles Lee
U	U	U	UU	11	**19b. TELEPHONE NUMBER** *(include area code)* 703-696-7779

Molecular Machine-Based Active Plasmonics

Award Number: FA9550-08-1-0349

Program Director: Dr. Charles Lee

PI: Tony Jun Huang (Penn State); co-PI: J Fraser Stoddart (Northwestern University)

Final Report

During this AFOSR project, PIs accomplished following milestones which could have significant impact in the field.

1. Synthesis and Functionalization of Molecular Motors

1.1. Acid-Base Actuation of [*c*2]Daisy Chains

We have accomplished (Figure 1) the synthesis, characterization, and mechanistic investigation of a mechanically interlocked, muscle-like, linear poly[*c*2]daisy chain.[8] The experimental results demonstrate that the functionalized [*c*2]daisy chains, along with their polymeric derivatives, undergo quantitative, efficient, and fully reversible switching processes in solution. Kinetic measurements reveal that the acid/base-promoted extension/contraction movements of the polymeric [*c*2]daisy chain are actually faster than those of its monomeric counterpart. These robust polymeric switchable materials set the stage for the development of smart materials and functional nanomachinery that are able to express correlated molecular motions.

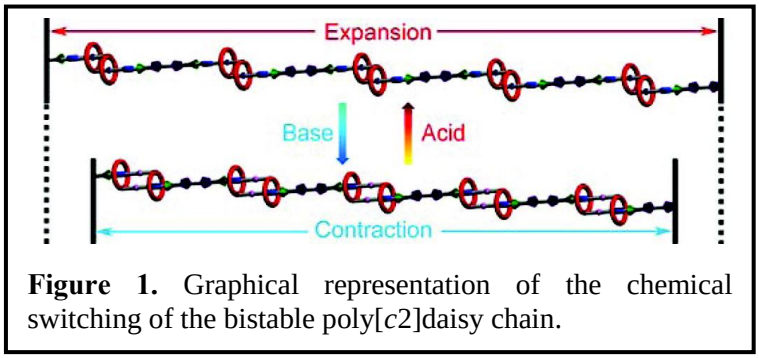

Figure 1. Graphical representation of the chemical switching of the bistable poly[*c*2]daisy chain.

A comprehensive review article has been published recently and has appeared on the cover of the first issue of the *Chemical Society Reviews* in 2010.[18] This article reviews the efforts, during the past two decades, of the incorporation of mechanical bonds into macromolecular materials. We believe that this review will be an excellent guide for the future research on mechanically interlocked polymers and their corresponding applications in functional materials.

1.2. Noncovalent Functionalization of Single-Walled Carbon Nanotubes

We have written a review article[9] for *Accounts of Chemical Research* describing the Stoddart Group's research on non-covalent functionalization of carbon nanotubes which promises to deliver a new generation of carbon nanotube hybrid-based integrated multifunctional sensors and devices based on switchable molecules. This outcome is essential for the development of carbon nanotube chemistry that interfaces with physics, materials, biology, and medical science.

2. Manufacturing of Plasmonic Nanostructures

2.1. Chemically Tuning the Localized Surface Plasmon Resonances of Gold Nanostructure Arrays

We demonstrated chemical etching of ordered Au nanostructure arrays to continuously tune their localized surface plasmon resonances (LSPR).[13] Real-time extinction spectra were recorded from both Au nanodisks and nanospheres immobilized on glass substrates when immersed in Au etchant. The time-dependent LSPR frequencies, intensities, and bandwidths were studied theoretically with discrete dipole approximations and the Mie solution, and they were correlated with the evolution of the etched Au nanostructures' morphology (as examined by atomic force microscopy). Since this chemical etching method can conveniently and accurately tune LSPR, it offers precise control of plasmonic properties and can be useful in applications such as surface-enhanced Raman spectroscopy and molecular resonance spectroscopy.

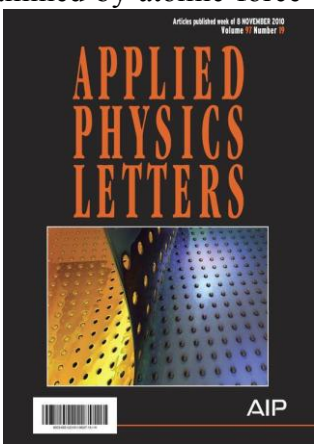

2.2. Complementary Patterned Metallic Membranes Produced Simultaneously by a Dual Fabrication Process

We have developed an efficient technique to fabricate optically thin metallic films with subwavelength patterns and their complements simultaneously.[27] By comparing the spectra of the complementary films, we show that Babinet's principle nearly holds for these structures in the optical domain. Rigorous full-wave simulations are employed to verify the experimental observations. It is further demonstrated that a discrete-dipole approximation can qualitatively describe the spectral dependence of the metallic membranes on the geometry of the constituent particles as well as the illuminating polarization. This work was featured as front cover article at the journal *Applied Physics Letters* (see the figure on right).

2.3. Scalable Manufacturing of Plasmonic Nanodisk Dimers and Cusp Nanostructures using Salting-out Quenching Method and Colloidal Lithography

We demonstrate a scalable, rapid, and inexpensive fabrication method based on the salting-out quenching technique and colloidal lithography for the fabrication of two types of nanostructures with large electric field: nanodisk dimers and cusp nanostructures. Our technique relies on fabricating polystyrene doublets from single beads by controlled aggregation and later using them as soft masks to fabricate metal nanodisk dimers and nanocusp structures. Both of these structures have a well-defined geometry for the localization of large electric fields comparable to structures fabricated by conventional nanofabrication techniques. We also show that various

parameters in the fabrication process can be adjusted to tune the geometry of the final structures and control their plasmonic properties. With advantages in throughput, cost, and geometric tunability, our fabrication method can be valuable in many applications that require plasmonic nanostructures with large electric fields.

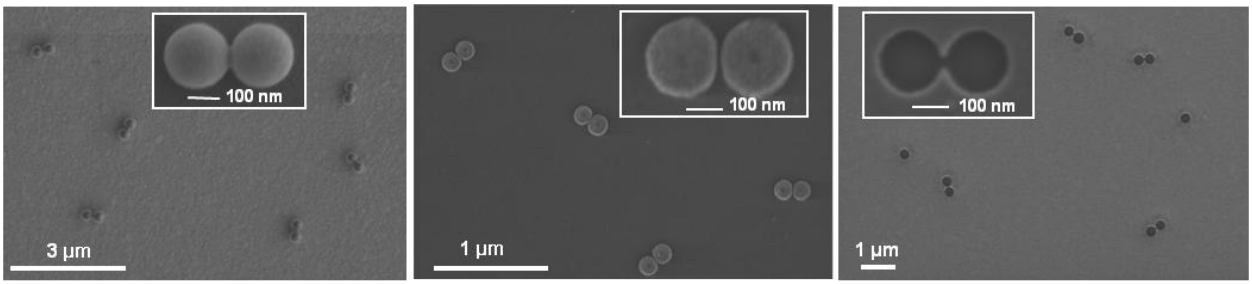

Figure 2. SEM images of nanoparticle dimmers and nanocusp structures.

3. Active Molecular Plasmonics: Controlling Plasmon Resonances with Molecular Switches

The Stoddart and Huang groups have demonstrated (Figure 3) a molecular-level active plasmonic device that can be operated by the switching of molecular machines based on bistable [2]rotaxanes which serve as a means to modulate the extinction coefficient of these molecules at particular wavelengths in the UV/Vis spectrum.[6] The reversible switching of the localized surface plasmon resonance (LSPR) of Au nanodisk arrays correlates with the chemically driven mechanical switching observed for surface-bound bistable [2]rotaxanes. This observation was supported by control experiments and a time-dependent density functional theory based, microscopic model. The active molecular plasmonic system demonstrated in our research can be differentiated from the existing systems in the following aspects: (i) the active components, namely bistable rotaxanes, are one of a unique class of molecules that can deliver controllable, reversible mechanical motions at the molecular level; (ii) the LSPR modulations observed in this work have been obtained for the first time with a monolayer (thickness: < 10 nm) of molecules, rather than from thin films or polymer matrices (thickness: > 50 nm). The results of this fundamental research could establish a technological basis for the production of a new class of molecular machine-based active plasmonic components for solid-state nanophotonic integrated circuits with the potential for low-energy and ultra-small operations. As a barometer of the significance of this work, it has been highlighted in *Nature Materials* and more than 30 public media sources including, *ScienceDirect, Science Mode, Nanotechnology Now, Foresight, PhysOrg, NanoWerk, AZoNanotechnology*).

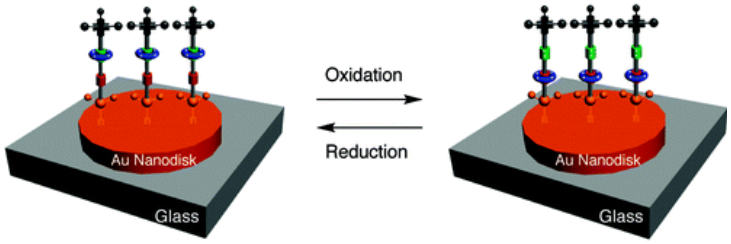

Figure 3. Schematic of working principle of the molecular-machine-based active plasmonics.

4. A Mechanical Actuator Driven Electrochemically by Artificial Molecular Muscles

We have shown (Figure 4)[7] that a gold microcantilever, coated with a monolayer of redox-controllable, palindromic bistable [3]rotaxane molecules (artificial molecular muscles) undergoes reversible deflections when subjected to alternating oxidizing and reducing electrochemical potentials. The microcantilever devices were prepared by precoating one surface with a gold film and allowing the ditholane-functionalized palindro-mic doubly bistable [3]rotaxane molecules to become adsorbed selectively onto one side of the microcantilevers, utilizing thiol-gold chemistry. An electrochem-ical cell was employed in the experiments and deflections were monitored both as a function of (i) the scan rate (≤ 20 mV s^{-1}) and (ii) the time for potential step experiments at oxidizing (> +0.4 V) and reducing (< +0.2 V) potentials. The different directions and magnitudes of the deflections for the microcantilevers, which were coated with artificial molecular muscles, were compared with: (i) data from nominally bare microcantilevers precoated with gold and (ii) those coated with two types of control compounds, namely, dumbbell molecules to simulate the redox-activity of the palindromic bistable [3]rotaxane molecules and inactive 1-dodecanethiol molecules. These experiments demonstrated that the bending of the gold cantilever is a direct consequence of the switching of the artificial molecular muscles and this switching process can be repeated over many cycles. It has also been shown that the microcantilevers deflect in one direction following oxidation, and in the opposite direction upon reduction. The ~550 nm deflections were calculated to be commensurate with forces per molecule of ~650 pN. The thermal relaxation that characterizes the device's deflection on return to its ground state is consistent with the double bistability associated with the palindromic [3]rotaxane and reflects a metastable contracted state. The use of the cooperative forces generated by these self-assembled, nanometer-scale artificial molecular muscles that are electrically wired to an external power supply constitutes a seminal step towards functional nanoelectromechanical systems (NEMS) based on artificial molecular muscles.

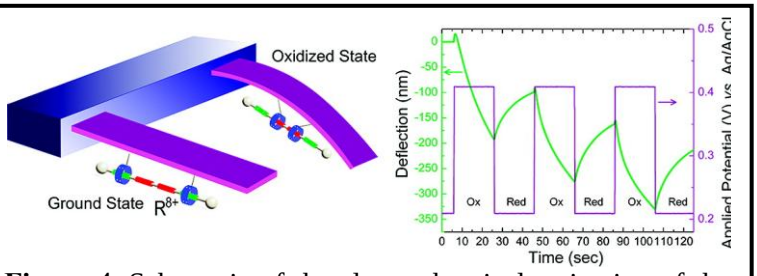

Figure 4. Schematic of the electrochemical activation of the palindromic bistable [3]rotaxane molecules and the reversible electrochemical oxidation and reduction of these molecules to produce the microcantilever deflection.

In addition, we have published a review article in the *MRS Bulletin* describing the three proven examples of nanomechanical actuation in artificial molecular systems, ranging from single-molecule switches, to rotaxane motors, and carbon nanotube-based artificial muscles.[16] We also discussed the principles behind driven motion and assembly at the molecular scale and recent advances in the field of molecular-level electromechanical machines, molecular motors, and artificial muscles. We described the challenges and successes in making these assemblies work cooperatively to function at larger scales. Ultimately, the ability to integrate molecular machine functionally for macroscale work will facilitate the development of multifunctional devices that can mimic and potentially surpass the complicated functions of natural systems.

5. Surface Enhanced Raman Spectroscopy (SERS) Properties of Molecular Motors

5.1. Effects of Intrinsic Fano Interference on Surface Enhanced Raman Spectroscopy: Comparison between Platinum and Gold

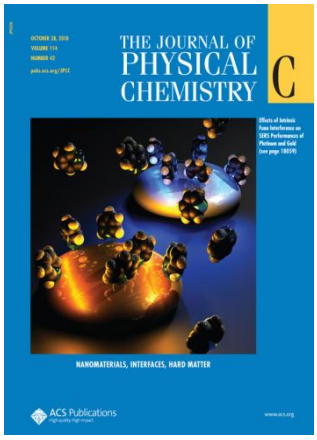

Using pyridine as a probe molecule, we performed Surface Enhanced Raman Spectroscopy (SERS) studies on platinum and gold nanodisk arrays at both plasmon resonant and off-plasmon resonant excitation wavelengths.[28] A large Raman cross-section enhancement factor (EF) of ~10^6 was obtained with plasmon resonant excitation on the Au array, and the EF decreases with off-resonant excitations. However, for Pt nanodisks the experimental EF is much smaller (~10^2), and not sensitive to excitation wavelength. Electric field intensities calculated in Au and Pt nanoparticles using the Discrete Dipole Approximation (DDA) with a dielectric function including or excluding inter-band transitions allowed us to explain the SERS EF differences at different excitation wavelengths. The observed SERS insensitivity to excitation wavelength in Pt was explained using Fano interference between the free plasmon electrons and continuum inter-band transitions. The importance of Fano interference was explored analytically in the electrostatic limit by varying the contribution from the inter-band transitions. This work was featured as front cover article at *Journal of Physical Chemistry C* (see the figure on left).

5.2. Turning On Resonance Raman – Surface Enhanced Raman Spectroelectrochemistry of a Tetrathiafulvalene Self-Assembled Monolayer

We have demonstrated (Figure 5) that both surface and resonance Raman enhancement can be exploited to elucidate chemical information in real time about the oxidation state of molecules at an electrode interface.[45] Electrochemical investigations indicate that non-idealities in the electrochemistry can be suppressed by diluting the surface concentration of redox-active compounds with an inert compound, suggesting that these non-ideal complications arise as a result of the interactions between neighboring tetrathiafulvalene (TTF) units. The surface-enhanced Raman spectroscopy and surface-enhanced resonance Raman scattering investigations revealed changes in vibrational frequencies of the TTF unit as a result of changes in oxidation state. Upon oxidation to the radical cation, the Raman spectrum of dithiolane-functionalized TTF is greatly enhanced by resonance between λ_{ex} and the electronic absorbance of the TTF unit. This highly sensitive contrast mechanism can be used to probe the state of TTF-bearing components in functional molecular electronic devices (MEDs). This nondestructive

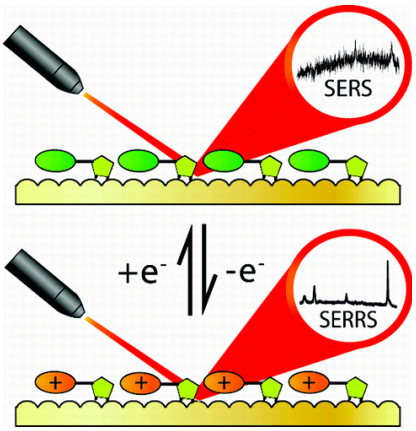

Figure 5. Schematic representation of the response of a self-assembled monolayer of a tetrathiafulvalene (green) derivative and its radical cation (orange) on a gold film monitored using Surface-enhanced Raman spectroscopy.

approach may allow the *in situ* chemical interrogations of molecular switching events at the interfaces of working MEDs, enabling the elucidation of the mechanistic processes involved in the response of switchable molecules to electronic stimulation.

6. Active Plasmonics Based on Liquid Crystals and Other Molecules

6.1. Light-Driven Plasmonic Switches Based on Au Nanodisk Arrays and Photoresponsive Liquid Crystals

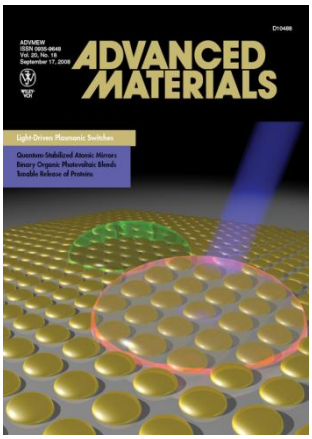

We have developed an optically controlled plasmonic switch using Au nanodisk arrays embedded in azobenzene-doped, photoresponsive liquid crystals (LCs).[1] The switch utilizes the photo-induced phase transition of azobenzene-doped LCs. This transition modulates the refractive indices of the LCs, thereby altering the localized surface plasmon resonance (LSPR) of the Au nanodisks. The experimental modulation of the LSPR matched well with theoretical modulation from discrete dipole approximation (DDA) calculations. We also examined how the angle of the incident light, power of the pump light, and wavelength of the probe light affect the performance of the switch. This work was featured as front cover article at the journal *Advanced Materials* (see the figure on right).

6.2. A frequency-addressed plasmonic switch based on dual-frequency liquid crystals

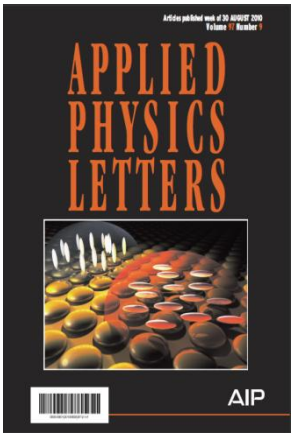

We demonstrated a frequency-addressed plasmonic switch by embedding a uniform gold nanodisk array into dual-frequency liquid crystals (DFLC).[30] The optical properties of the hybrid system were characterized by extinction spectra of localized surface plasmon resonances (LSPRs). The LSPR peak was tuned using a frequency-dependent electric field. A ~4 nm blue-shift was observed for frequencies below 15 kHz, and a 23 nm red-shift was observed for frequencies above 15 kHz. The switching time for the system was ~40 ms. This DFLC-based active plasmonic system demonstrates an excellent, reversible, frequency-dependent switching behavior and could be used in future integrated nanophotonic circuits. This work was featured as front cover article at the journal *Applied Physics Letters* (see the figure on left).

6.3. All-Optical Modulation of Localized Surface Plasmon Coupling in a Hybrid System Composed of Photo-Switchable Gratings and Au Nanodisk Arrays

We carry out a real-time study of all-optical modulation of localized surface plasmon resonance (LSPR) coupling in a hybrid system that integrates a photo-switchable optical grating with a Au nanodisk array.[28] In this hybrid system, the photo-switchable grating was produced from azo-dye-doped holographic polymer-disperse liquid crystals (HPDLC). This hybrid system enables us to investigate two important interactions: 1) LSPR-enhanced diffraction of the grating, and 2) diffraction-mediated LSPR of the Au nanodisk array. The physical mechanism underlying these

interactions was also analyzed and experimentally confirmed. With its advantages in cost-effective fabrication, easy integration, and all-optical control, the hybrid system described in this work could be valuable in many nanophotonic applications. This work was featured as front cover article at *Journal of Physical Chemistry C* (see the figure on right).

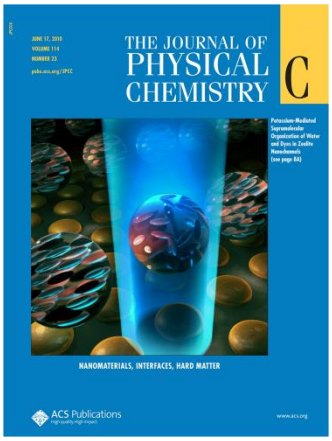

6.4. Dynamically Tuning Plasmon–Exciton Coupling in Arrays of Nanodisk–J-aggregate Complexes

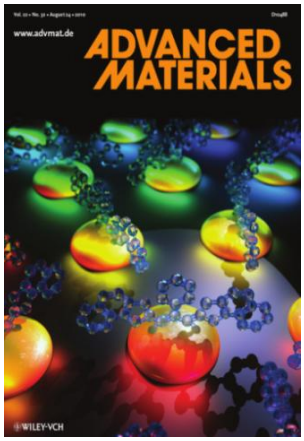

We demonstrate dynamic tuning of plasmon-exciton resonant coupling in arrays of nanodisk–J-aggregate complexes.[34] The angle-resolved spectra of an array of bare Au nanodisks exhibit continuous shifting of localized surface plasmon resonances. This characteristic enables the production of real-time, controllable spectral overlaps between molecular resonance and plasmonic resonance. In this work we explore resonant interaction strength as a function of spectral overlap. In experiments where we changed the incident angle of a probe light, the coupling strength changed; this result matched with the simulated data based on a coupled dipole approximation method. This work was featured as front cover article at the journal *Advanced Materials* (see the figure on right).

6.5. Surface acoustic wave driven light shutters using polymer-dispersed liquid crystals

We have demonstrated a surface acoustic wave (SAW)-driven light shutter using polymer-dispersed liquid crystals (PDLCs).[44] Our experiments showed that upon applying a SAW, the PDLC film switched from a non-transparent state to a transparent state. The working mechanism was analyzed theoretically and the acousto-optic properties of the PDLC film were characterized experimentally. This switching behavior is due to the acoustic streaming-induced realignment of liquid crystal (LC) molecules as well as SAW-induced thermal diffusion. Such a SAW-driven device shows an excellent performance in terms of imaging quality and optical contrast, which is important for display applications and smart windows. This new driving scheme could be widely used for PDLC-based photonic devices. This work was featured as front cover article at the journal *Advanced Materials* (see the figure on right).

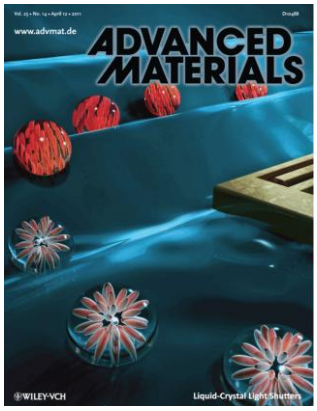

Publications Resulted from this AFOSR Program

1. Light-driven plasmonic switches based on Au nanodisk arrays and photoresponsive liquid crystals (V.K.S. Hsiao, Y.B. Zheng, B.K. Juluri, T.J. Huang), *Adv. Mater*. **2008**, *20*, 3528-3522. **C*over Article***
2. Systematic investigation of localized surface plasmon resonance of long-range ordered Au nanodisk arrays (Y.B. Zheng, B.K. Juluri, X. Mao, T.R. Walker, T.J. Huang), *J. Appl. Phys*. **2008**, *103*, 014308.
3. Recent developments in artificial molecular machine-based active nanomaterials and nanosystems (T.J. Huang), *MRS Bulletin* **2008**, *33*, 226-231.
4. Effects of geometry and composition on charge-induced plasmonic shifts in gold nanoparticles (B.K. Juluri, Y.B. Zheng, D. Ahmed, L. Jensen, T.J. Huang), *J. Phys. Chem. C* **2008**, *112*, 7309-7312.
5. A bistable poly[2]catenane forms nanosuperstructures (M.A. Olson, A.B. Braunschweig, L. Fang, T. Ikeda, R. Klajn, A. Trabolsi, C.A. Mirkin, B.A. Grzybowski, J.F. Stoddart), *Angew. Chem. Int. Ed.* **2009**, *48*, 1792–1797.
6. Active molecular plasmonics: Controlling plasmon resonances with molecular switches (Y.B. Zheng, Y.-W. Yang, L. Jensen, L. Fang, B.K. Juluri, A.H. Flood, P.S. Weiss, J.F. Stoddart, T.J. Huang), *Nano Lett.* **2009**, *9*, 819–825.
7. A mechanical actuator driven electrochemically by artificial molecular muscles (B.K. Juluri, A.S. Kumar, Y. Liu, T. Ye, Y.-W. Yang, A.H. Flood, L. Fang, J.F. Stoddart, P.S. Weiss, T.J. Huang), *ACS Nano* **2009**, *3*, 291–300.
8. Acid-base actuation of [c2]daisy chains (L. Fang, M. Hmadeh, J. Wu, M.A. Olson, J.M. Spruell, A. Trabolsi, Y.-W. Yang, M. Elhabri, A.-M. Albrecht-Gary, J.F. Stoddart), *J. Am. Chem. Soc.* **2009**, *131*, 7126–7134.
9. Noncovalent functionalization of single-walled carbon nanotubes (Y.-L. Zhao, J.F. Stoddart) *Acc. Chem. Res.* **2009**, *42*, 1161–1171.
10. Coupling between molecular and plasmonic resonances: effect of molecular absorbance (B.K. Juluri, M. Lu, Y.B. Zheng, L. Jensen, T.J. Huang), *J. Phys. Chem. C* **2009**, *113*, 18499–18503.
11. Propagation of designer surface plasmons in structured conductor surfaces with parabolic gradient index (B.K. Juluri, S-C. S. Lin, T.R. Walker, L. Jensen, T.J. Huang), *Opt. Exp.* **2009**, *17*, 2997-3006.
12. Gradient-index phononic crystals (S.-C. S. Lin, T.J. Huang, J.-H. Sun, T.-T. Wu), *Phys. Rev. B* **2009**, *79*, 094302.
13. Chemically tuning the localized surface plasmon resonances of gold nanostructure arrays (Y.B. Zheng, L.L. Jensen, W. Yan, T.R. Walker, B.K. Juluri, L. Jensen, T.J. Huang), *J. Phys. Chem. C* **2009**, *113*, 7019-7024..
14. Electrically switchable phase-type fractal zone plates and fractal photon sieves (Y.J. Liu, H.T. Dai, X.W. Sun, T.J. Huang), *Opt. Exp.* **2009**, *17*, 12418-12423.

15. Optically switchable gratings based on azo-dye-doped, polymer-dispersed liquid crystals (Y.J. Liu, Y.B. Zheng, J. Shi, H. Huang, T.R. Walker, T.J. Huang), *Opt. Lett.* **2009**, *34*, 2351-2353.
16. Molecular, supramolecular, and macromolecular motors and artificial muscles (D. Li, W.F. Paxton, R.H. Baughman, T.J. Huang, J.F. Stoddart, P.S. Weiss), *MRS Bulletin* **2009**, *34*, 671–681.
17. Radically enhanced molecular recognition (A. Trabolsi, N. Khashab, A.C. Fahrenbach, D.C. Friedman, M.T. Colvin, K.K. Cotí, D. Benitez, E. Tkatchouk, J.-C. Olsen, M.E. Belowich, R. Carmielli, H.A. Khatib, W.A. Goddard III, M.R. Wasielewski, J.F. Stoddart), *Nature Chem.* **2010**, *2*, 42–49.
18. Mechanically bonded macromolecules (L. Fang, M.A. Olson, J.F. Stoddart), *Chem. Soc. Rev.* **2010**, *39*, 17–29. ***Cover Article***
19. A metal-organic framework replete with ordered donor-acceptor catenanes (Q. Li, W. Zhang, O.Š. Miljanić, C.B. Knobler, J.F. Stoddart, O.M. Yaghi), *Chem. Commun*. **2010**, *46*, 380–382.
20. A tristable [2]pseudo[2]rotaxane (A. Trabolsi, A.C. Fahrenbach, A.I. Share, D.C. Friedman, T.B. Gasa, S.K. Dey, N.M. Khashab, S. Saha, I. Aprahamian, H.A. Khatib, A.H. Flood, J.F. Stoddart), *Chem. Commun*. **2010**, *46*, 871–873.
21. A redox-switchable [2]rotaxane in a liquid-crystalline state (T. Yasuda, K. Tanabe, T. Tsuji, K.K. Cotí, I Aprahamian, J.F. Stoddart, T. Kato), *Chem. Commun.* **2010**, *46*, 1224–1226.
22. Robust dynamics (H. Deng, M.A. Olson, J.F. Stoddart, O.M. Yaghi), *Nature Chem.* **2010**, *2*, 439–443.
23. Isolation by crystallization of translational isomers of a bistable donor-acceptor [2]catenane (C. Wang, M.A. Olson, L. Fang, D. Benítez, E. Tkatchouk, S. Basu, D. Zhang, D. Zhu, W.A. Goddard III, J.F. Stoddart), *Proc. Natl. Acad. Sci. USA* **2010**, *107*, 13991–13996.
24. Highly stable tetrathiafulvalene radical dimers in [3]catenanes (J.M. Spruell, A. Coskun, D.C. Friedman, R.S. Forgan, A.A. Sarjeant, A. Trabolsi, A.C. Fahrenbach, G. Barin, W.F. Paxton, S.K. Dey, M.A. Olson, D. Benítez, E. Tkatchouk, M.T. Colvin, R. Carmielli, S.T. Caldwell, G.M. Rosair, S.G. Hewage, F. Duclairoir, J.L. Seymour, A.M.Z. Slawin, W.A. Goddard III, M.R. Wasielewski, G. Cooke, J.F. Stoddart), *Nature Chem.* **2010**, *2*, 870–879.
25. Molecular machines drive smart drug delivery (Y.B. Zheng, B. Kiraly, T.J. Huang), *Nanomedicine* **2010**, *5*, 1309-1312.
26. Beam aperture modification and beam deflection using gradient-index photonic crystals (M. Lu, B.K. Juluri, S.-C. S. Lin, B. Kiraly, T. Gao, T.J. Huang), *J. Appl. Phys.* **2010**, *108*, 103505.
27. Characterization of complementary patterned metallic membranes produced simultaneously by a dual fabrication process (Q. Hao, Y. Zeng, X. Wang, Y. Zhao, B. Wang, I.-K. Chiang, D.H. Werner, V. Crespi, T.J. Huang), *Appl. Phys. Lett.* **2010**, *97*, 193101. ***Cover Article***
28. Effects of intrinsic fano interference on surface enhanced Raman spectroscopy: comparison between platinum and gold (Q. Hao, B.K. Juluri, Y.B. Zheng, B. Wang, I.-K. Chiang, L. Jensen, V. Crespi, P.C. Eklund, T.J. Huang), *J. Phys. Chem. C* **2010**, *114*, 18059–18066. ***Cover Article***

29. Beam bending via plasmonic lenses (Y. Zhao, S.-C. S. Lin, A.A. Nawaz, B. Kiraly, Q. Hao, Y. Liu, T.J. Huang), *Opt. Exp.* **2010**, *18*, 23458-23465.
30. A frequency-addressed plasmonic switch based on dual-frequency liquid crystal (Y.J. Liu, Q. Hao, J. S.T. Smalley, J. Liou, I.C. Khoo, T.J. Huang), *Appl. Phys. Lett.* **2010**, *97*, 091101. ***Cover Article***
31. Light-driven artificial molecular machines (Y.B. Zheng, Q. Hao, Y.-W. Yang, B. Kiraly, I.-K. Chiang, T.J. Huang), *J. Nanophotonics* **2010**, *4*, 042501.
32. Photonic crystal composites-based wide-band optical collimator (J. Shi, B.K. Juluri, S.-C. S. Lin, M. Lu, T. Gao, T.J. Huang), *J. Appl. Phys.* **2010**, *108*, 043514.
33. Ordered Au nanodisk and nanohole arrays: fabrication and applications (Y.B. Zheng, B.K. Juluri, T.J. Huang), *ASME Journal of Nanotechnology in Engineering and Medicine* **2010**, *1*, 031011.
34. Dynamically tuning plasmon-exciton coupling in arrays of nanodisk-J-aggregate complexes (Y.B. Zheng, B.K. Juluri, L.L. Jensen, D. Ahmed, M. Lu, L. Jensen, T.J. Huang), *Adv. Mater.* **2010**, *22*, 3603-3607. ***Cover Article***
35. Solution-phase counterion effects in supramolecular and mechanostereochemical systems (T.B. Gasa, C. Valente, J.-F. Stoddart), *Chem. Soc. Rev.* **2011**, *40*, 57–78.
36. Syntheses and dynamics of donor–acceptor [2]catenanes in water (L. Fang, S. Basu, C.-H. Sue, A.C. Fahrenbach, J.F. Stoddart), *J. Am. Chem. Soc.* **2011**, *133*, 396–399.
37. Microcontact click printing for templating ultrathin films of metal–organic frameworks (J.J. Gassensmith, P.M. Erne, W.F. Paxton, C. Valente, J.F. Stoddart), *Langmuir* **2011**, *27*, 1341–1345.
38. Dual stimulus switching of a [2]catenane in water (L. Fang, C. Wang, A.C. Fahrenbach, A. Trabolsi, Y.Y. Botros, J.F. Stoddart), *Angew. Chem. Int. Ed.* **2011**, *50*, 1805–1809.
39. Optical and vibrational properties of toroidal carbon nanotubes (F. Beuerle, C. Herrmann, A.C. Whalley, C. Valente, A. Gamburd, M.A. Ratner, J.F. Stoddart), *Chem. Eur. J.* **2011**, *17*, 3868–3875.
40. Mechanically stabilized tetrathiafulvalene radical dimers (A. Coskun, J.M. Spruell, G. Barin, A.C. Fahrenbach, R.S. Forgan, M.T. Colvin, R. Carmielli, D. Benítez, E. Tkatchouk, D.C. Friedman, A.A. Sarjeant, M.R. Wasielewski, W.A. Goddard III, J.F. Stoddart), *J. Am. Chem. Soc.* **2011**, *133*, 4538–4547.
41. Frequency-addressed tunable transmission in optically thin metallic nanohole arrays with dual-frequency liquid crystals (Q. Hao, Y. Zhao, B.K. Krishna Juluri, B. Kiraly, J. Liou, I.C. Khoo, T.J. Huang), *J. Appl. Phys* .**2011**, *109*, 084340.
42. Tunable phononic crystals with anisotropic inclusions (S.-C. S. Lin, T.J. Huang), *Phys. Rev. B* **2011**, *83*, 174303.
43. All-optical modulation of localized surface plasmon coupling in a hybrid system composed of photo-switchable gratings and Au nanodisk arrays (Y.J. Liu, Y.B. Zheng, J. Liou, I.-K. Chiang, I.C. Khoo, T.J. Huang), *J. Phys. Chem. C* **2011**, *115*, 7717–7722. ***Cover Article***

44. Surface acoustic wave driven light shutters using polymer-dispersed liquid crystals (Y.J. Liu, X. Ding, S.-C. S. Lin, J. Shi, I.-K. Chiang, T.J. Huang), *Adv. Mater.* ***2011***. *23*, 1656-1659. ***Cover Article***

45. Turning on resonance Raman – surface enhanced Raman spectroelectrochemistry of a tetrathiafulvalene self-assembled monolayer (W. F. Paxton, S. L. Kleinman, A. N. Basuray, J. F. Stoddart, R. P. Van Duyne), *J. Phys. Chem. Lett.* **2011**, *2*, 1145–1149.